Measurements of anchoring energy of a nematic liquid crystal, 4-cyano-4′-*n*-pentylbiphenyl, on Langmuir-Blodgett films of dipalmitoyl phosphatidylcholine

U. Kühnau, A. G. Petrov,* G. Klose, and H. Schmiedel
Fakultät für Physik und Geowissenschaften, Universität Leipzig, Linnéstrasse 5, D-04103 Leipzig, Germany
(Received 23 June 1997; revised manuscript received 18 November 1997)

The Langmuir-Blodgett technique was used for deposition of monolayer lipid films of dipalmitoyl phosphatidylcholine (DPPC) on glass with a variable surface density of lipid molecules. In a certain range of surface density these surfaces oriented homeotropically the highly polar nematic liquid crystal of 4-cyano-4′-*n*-pentylbiphenyl (5CB). Optical transmission curves of liquid crystal layers sandwiched between orienting lipid monolayers were recorded versus magnetic field with high accuracy. They were further converted into optical retardation and fitted by a complete theory of the transition containing anchoring strength as a parameter. Independent measurements of refractive indices of 5CB were also performed by the prism method. Anchoring energies thus obtained showed a nonmonotonic behavior with increasing packing density of DPPC monolayers and a pronounced minimum around 0.82 nm^2 per molecule. This is explained by a complete theory of surface anchoring including steric, electric, flexoelectric, and notably surface polarization coupling mechanisms. The last one stands for surface polarized layers at the liquid-crystal interfaces interacting with surface electric field due to lipid molecules. The competition of these mechanisms leads to an initial dehancement followed by an enhancement of the anchoring strength at monotonically increasing DPPC packing density. Surface polarization evaluated from the experimental data is in good correspondence with molecular parameters. [S1063-651X(99)08701-2]

PACS number(s): 61.30.Eb

INTRODUCTION

Organized layers of biphilic molecules (lipids, fatty acids, surfactants, monomer, or polymer ones) on solid supports have been used for a long time as orienting substrates for nematic liquid crystals (NLC's) [1,2]. They are known to influence NLC orientation at the boundary in a specific way depending on surface molecular density, surface charge and/or dipole of the hydrophilic head group, number of hydrophobic tails, tail length, temperature, etc. This phenomenon is known as liquid crystal anchoring (homeotropic, planar, or tilted).

The Langmuir-Blodgett (LB) technique offers a straightforward way of varying the surface molecular density by compressing or expanding the precursor monolayer on the air/water interface. It has been known for a long time that the quality of anchoring depends strongly on LB film density: expanded layers result in much better homeotropic orientation than compressed ones, attributed to the presence of molecular vacancies, ''holes,'' in them [3–5]. However, quantitative measurements of anchoring strength in dependence of packing density are still not available in the literature, and thus the ''hole'' concept is not quantified.

Furthermore, it should be emphasized that the ''holes'' are not fully preconditioned by the LB film itself, but arise in a specific interaction process between the LB monolayer and liquid crystal (LC) molecules, as our experiments on mixed DPPC/5CB Langmuir films demonstrate [6,7]. In that sense the ability of LC molecules to occupy the ''holes'' reflects the ability of a NLC to ''dissolve'' in the LB film, i.e., the ability of the mixed LC-surfactant Langmuir film to form a new, two-dimensional (2D) mixed phase at the interface [7]. On the other hand, ''holes'' may also arise in a process of LB film desorption, which means dissolving DPPC molecules in the bulk of NLC's.

Moreover, precise numerical values of anchoring energy are of considerable interest both for the surface liquid crystal physics and for technical applications. However, in dependence on experimental methods for measurement and surface preparation, anchoring energy values may vary by orders of magnitude [8]. In addition, in case of strong anchoring, the exactness of surface energy coefficient depends critically on the accuracy of different LC cell parameters such as refractive indices, cell thickness, or bulk elastic constants.

In our experiments, we prepared an extended set of LC cells differing in surface density of orienting LB films. Optical transmission curves of 5CB sandwiched between orienting lipid monolayers were recorded versus magnetic field (Fréedericksz transition [9]). To fit the experimentally obtained optical retardations, we used a numerical method for the solution of the Euler-Lagrange equation which is quite different from the multidimensional shooting method usually applied in solving the nonlinear boundary-value problem [10]. The method presented here is easier to accomplish and exhibits shorter computer times. The difficulties in the determination of surface energy mentioned above were solved by taking into account the data of the whole set in the fitting procedure. In this way, it was possible to detect small differences in surface energy between the cells of the set. The thickness of the filled cells was measured by the crystal rotation method. Optical refractive indices of 5CB were ob-

*Present address: Biomolecular Layers Department, Institute of Solid State Physics, Bulgarian Academy of Sciences, 72 Tzarigradsko chaussee, 1784 Sofia, Bulgaria.

 ©1999 The American Physical Society

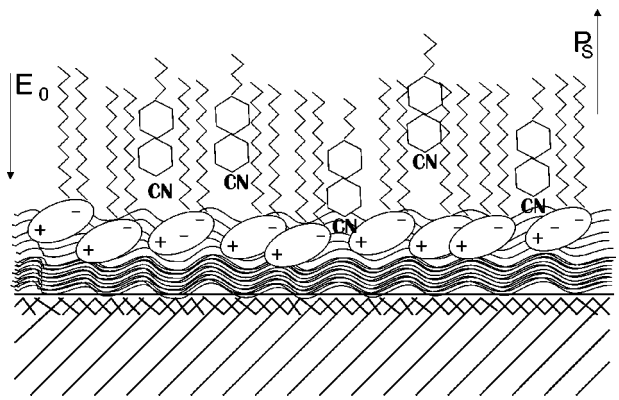

FIG. 1. Schematic representation of NLC-LB film interaction in the case of the DPPC-5CB interface. A thin film of trapped water between glass substrate and DPPC head groups is assumed. 5CB molecules penetrate the DPPC monolayer in an orienting fashion, aiming with their highly polar CN group towards a hydrophilic glass surface. In this way 5CB erects alkyl chains of DPPC that are normally tilted [6], and acquires a polarized dipolar surface layer due to the surface biphilic field [14]. Lipid heads may carry partial electric charge, giving rise also to a surface electric field.

tained by means of a higher accuracy modification of the prism method using an orienting magnetic field.

THEORY

We start with an outline of the theory [11–13] in order to provide a general framework for our discussion. We consider a hydrophilic glass substrate covered by an LB monolayer of lipid molecules with area density n_{LB} (Fig. 1). The steric part of the anchoring energy, W_0, we regard as a constant in the range of densities provided by the LB technique (from 1.0×10^{18} to 1.5×10^{18} m^{-2}).

We also stress that 5CB molecules enter the LB film in a polar fashion (Fig. 1), which gives rise to a surface polarized layer of density P_S of the nematic in the immediate contact with the LB film [13–15].

Furthermore, we assume that due to the contact of lipid molecules with glass, some kind of charge separation takes place between the glass surface and the lipid monolayer (its mechanism will be specified later on), or, alternatively, that each lipid molecule brings about (on average) some small partial charge (cf. [13]). Thus, we hypothesize that the amount of surface charge is explicitly related to lipid density (see the Discussion).

After making contact with the liquid crystal, the surface electric field E_0 originating from surface charges will no longer be confined between glass and the DPPC monolayer, but will rather penetrate the bulk to some extent, because of the onset of counterion mobility. It is very important to elucidate the extent of field penetration or, conversely, the extent of field screening. The screening by the ions present in the bulk of a weak electrolyte (i.e., the liquid crystal) is well known and sufficiently well described by the Debye-Hückel theory [16]. The limit of vanishing bulk ion concentration n_∞ (far from the walls) is less familiar. The screening is then accomplished by the counterions of the surface charged groups. Thus, we take the limit $n_\infty\to0$, i.e., $\psi_0\to\infty$ of the Gouy-Chapman solution [Eq. (12.39) in [16]] of the nonlinear Poisson-Boltzmann equation and of the Grahame equation [Eq. (12.30) in [16]]. In this way we obtain the distance dependence of the surface field with no bulk screening in the following, not very common, form:

$$E(z)=\frac{\sigma}{\epsilon\epsilon_0}\frac{1}{1+z/\lambda_S}=\frac{E_0}{1+z/\lambda_S}, \tag{1}$$

where z is a coordinate, normal to the glass plane, σ is the surface charge density, ϵ is an appropriate dielectric constant of the liquid crystal (e.g., $\epsilon_{||}$ for a homeotropically oriented LC), ϵ_0 is the absolute dielectric permittivity of free space, and λ_S is a characteristic length of surface screening:

$$\lambda_S=\frac{2\epsilon\epsilon_0 k_B T}{q_e\sigma}, \tag{2}$$

where q_e is the proton charge and k_BT is the thermal energy. We see that unlike the case of bulk screening, Eq. (1) represents a fractional rational function, instead of an exponential one. Surface screening length λ_S (introduced here) plays the role of the Debye screening length, λ_D:

$$\lambda_D=\sqrt{\frac{\epsilon\epsilon_0 k_B T}{2q_e^2 n_\infty}}, \tag{3}$$

which accounts for the bulk screening (cf. [16]). A better insight into the meaning of λ_S can be obtained by noting that it equals the distance up to which thermal energy could pull an elementary charge against the surface electric field of the charged plane ($E_0=\sigma/\epsilon\epsilon_0$). Comparing λ_S and λ_D we can see that bulk screening takes over surface screening when bulk ion concentration exceeds a limiting value:

$$n_\infty^{\lim}=\frac{\sigma^2}{8\epsilon\epsilon_0 k_B T}. \tag{4}$$

If we assume a (very low) surface charge density of one elementary charge per 1000 lipid molecules, with an area per DPPC molecule at close packing of about 0.5 nm^2, we can calculate from Eq. (4) (using $\epsilon=18$, see below) the value of 2.0×10^{22} m^{-3} or, in charge units, 3200 $\mathrm{C/m}^3$. If we compare this to the usual values of ion concentration for pure liquid crystals, i.e., 6 $\mathrm{C/m}^3$ [17], we see that in pure materials surface screening is much more important than bulk screening, even at such very low surface charge values : under the same conditions $\lambda_S=25$ nm [from Eq. (2)] while $\lambda_D=580$nm [17].

Surface electric field is an important source of LB-LC coupling with three main components: dielectric, flexoelectric, and polarization [11–13]. However, in view of the present finding that this field is always effectively screened (especially in pure LC materials) by the surface counterions (cf. also [18] in this respect), no substantial field penetration in the bulk could be expected and thus dielectric coupling considered earlier to be of primary importance should rather be considered negligible (see below).

Now, with a surface field in the form of Eq. (1) we can get from [13] for the surface energy function the following expression:

$$F_{\text{surf}}=\frac{1}{2}\left(\frac{1}{2}\lambda_S\Delta\epsilon\epsilon_0E_0^2+eE_0+W_0\right)\sin^2\theta_S-P_SE_0\cos\theta_S, \tag{5}$$

where $\Delta\epsilon$ is dielectric anisotropy of the liquid crystal, e $(=e_{1z}+e_{3x})$ is its total flexoelectric coefficient, P_S is the surface polarization, and θ_S is the angle between the surface director and the substrate normal (z direction). In the limit of small θ_S, this expression simplifies to

$$F_{\text{surf}}=\frac{1}{2}\left(\frac{1}{2}\lambda_S\Delta\epsilon\epsilon_0E_0^2+eE_0+P_SE_0+W_0\right)\theta_S^2=\frac{1}{2}W_S\theta_S^2. \tag{6}$$

While the first dielectric term in the brackets appears quadratic in the surface field, it is actually linear in view of Eq. (2). Then we get

$$W_S=\left(\frac{\Delta\epsilon\epsilon_0k_BT}{q_e}+e+P_S\right)E_0+W_0. \tag{7}$$

If we now estimate the first term in the parentheses (with $k_BT/q_e=25$ mV and $\Delta\epsilon=12$ [19]) we get a value of 2.7×10^{-12} C/m. Indeed, compared to $e\approx1\times10^{-11}$ C/m [20] and $P_S\propto10^{-10}$ C/m (see the Discussion), this term could safely be neglected.

For further discussion it is very important to note that surface polarization is also dependent on monolayer lipid density, because the number of polarly ordered 5CB molecules depends on the free available area in the LB film (i.e., the total area of the incorporated LC molecules; cf. Fig. 1).

Having realized that anchoring strength depends on the details of surface electric field coupling to the LC, we have chosen the magnetic Fréedericksz transition as a method for measuring effective anchoring energy. Obviously, the electric Fréedericksz transition would disturb this coupling by shifting surface charge equilibrium and could produce rather different results.

Magnetic deformation of a LC layer (of thickness d) was described by minimization of the free elastic energy functional containing surface terms:

$$F=\int_0^d(f_{\text{elast}}+f_{\text{magn}})dz+F_{\text{surf}(0)}+F_{\text{surf}(d)}. \tag{8}$$

Surface energy was used in Rapini-Papoular form [21]: $F_{\text{surf}}=1/2W_S\sin^2\theta_S$, with W_S from Eq. (7). Such a form is easier to handle than that given by Eq. (5). Its use is justified providing that deformation angle θ_S is small enough. Elastic and magnetic energy densities have their familiar form [9].

$$f_{\text{elast}}=\frac{1}{2}(K_{11}\sin^2\theta+K_{33}\cos^2\theta)\left(\frac{d\theta}{dz}\right)^2,$$
$$f_{\text{magn}}=-\frac{1}{2}\mu_0\chi_aH^2\sin^2\theta, \tag{9}$$

where K_{33} is the bend elastic constant, K_{11} is the splay elastic constant, χ_a is the diamagnetic anisotropy, and μ_0 is the absolute magnetic permittivity of free space. Integration of the corresponding Euler-Lagrange equations for the function $\theta(z)$ under the constraint of the (symmetric) boundary conditions leads to (θ_S is the angle at the surface).

$$\frac{1}{\kappa}\frac{H}{H_S}=\frac{2}{\pi}\int_0^{\psi(\theta_S)}\sqrt{\frac{1+\eta(1+\tan^2\psi)\sin^2\theta_S\cos^2\theta}{1-(1+\tan^2\psi)\sin^2\theta_S\cos^2\theta}}d\theta, \tag{10}$$

where

$$\psi(\theta_S)=\arctan\left[\frac{H_S}{H}\sqrt{\frac{1-\sin^2\theta_S}{1+\eta\sin^2\theta_S}}\right],$$

$$\eta=\frac{K_{11}-K_{33}}{K_{33}},\quad \kappa=\frac{\pi K_{33}}{W_Sd},$$

$$H_F=\frac{\pi}{d}\sqrt{\frac{K_{33}}{\mu_0\chi_a}},\quad\text{and}\quad H_S=\frac{H_F}{\kappa}=\frac{W_S}{\sqrt{\mu_0\chi_aK_{33}}}.$$

For any given value of W_S, Eq. (10) provides a relationship between θ_S and the ratio of the applied magnetic field H to the ideal Fréedericksz threshold H_F, which is the threshold field for infinitely strong anchoring. Equation (10) was solved numerically (Fig. 2) and χ_a was taken from [22]. For fitting to the experiment, the deformation described by Eq. (10) must be translated into the optical retardation curve:

$$\Delta(H)=\frac{4n_od}{\lambda}\frac{H_F}{H}\int_0^{\psi(\theta_S)}\sqrt{\frac{1+\eta(1+\tan^2\psi)\sin^2\theta_S\cos^2\theta}{1-(1+\tan^2\psi)\sin^2\theta_S\cos^2\theta}}\left[\frac{1}{\sqrt{1-\zeta(1+\tan^2\psi)\sin^2\theta_S\cos^2\theta}}-1\right]d\theta, \tag{11}$$

where $\Delta=2\pi(\overline{n_e}-n_o)d/\lambda$ is the optical retardation (in rad), λ is the light wavelength, $\zeta=1-(n_o^2/n_e^2)$, and n_o,n_e are the ordinary and extraordinary index of refraction.

EXPERIMENT

LC sandwich cells were made by highly transparent B270 cronglass plates, used for LC devices (Gebr. Rettberg GmbH, Germany). These were cleaned for 25 min with a glass cleaning mixture (Hellmanex II, 2% in water, Hellma GmbH, Germany) at 80 °C. Subsequently, the substrates were rinsed 10 times with highly purified water (ELGA Ultra High Quality II, UK) and once more cleaned for 25 min in saturated chromosulfuric acid at 80 °C. Finally, the substrates were again rinsed 10 times with highly purified water

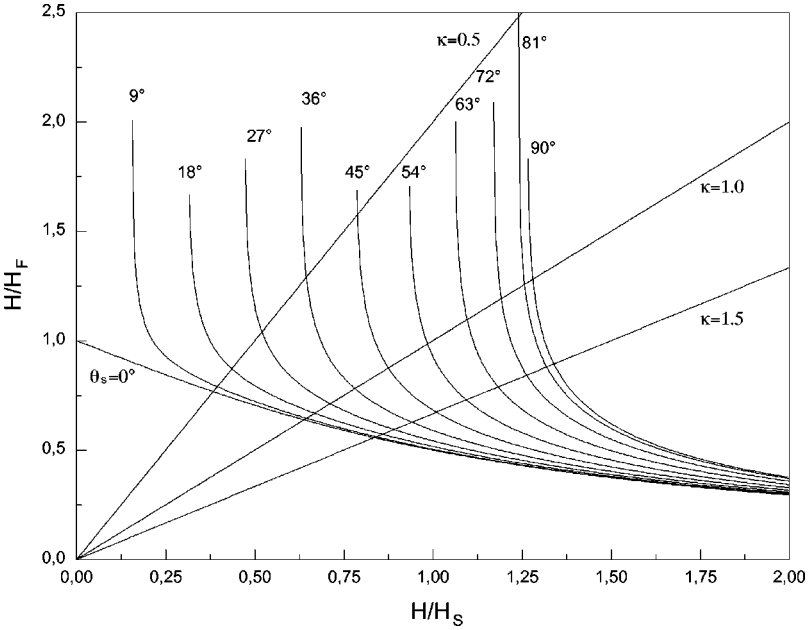

FIG. 2. Graphical solution of Eq. (10) in the text. Straight lines from the origin represent the left-hand side of Eq. (10) for the indicated values of κ and curved lines represent the integral on the right-hand side for a number of values of the surface angle θ_S. The crossing point of any straight line with the line $\theta_S=0$ gives the relative threshold field for the corresponding anchoring energy, while that with $\theta_S=90°$ represents the saturation field. The graph corresponds to $\eta=-0.375$.

and immediately used for LB film deposition. By means of a dynamic surface tensiometer (DST 9025, Nima Technology Ltd, UK), advancing and receding contact angles for water of less than 4° were obtained with these cleaned plates.

LB films for liquid crystal alignment were made from the synthetic lipid DPPC (>99% purity, Sigma). DPPC was dissolved in chloroform (>99% purity, Merck, Germany) and spread on the aqueous subphase of the LB trough (Nima 622D2, Nima Technology Ltd, UK) after glass substrates had been immersed. The compression rate of the lipid monolayer was on average 0.03 $nm^2\,molecule^{-1}\,min^{-1}$. DPPC monolayers were deposited on glass substrates at areas per molecule in the range from 0.7 nm^2 to 1.0 nm^2. Deposition was always performed at 26 °C. All these areas then correspond to the expanded part of the π-A isotherm, above the beginning of condensation (Fig. 5). The withdrawing speed of glass slides was 3 mm/min. Immediately after monolayer transfer, two glass plates were mounted in a cell holder with antiparallel pulling directions, using spacers in the range of 16 μm to 23 μm. The parallelism was checked by a laser beam. After filling the cells with the nematic 5CB (Merck, Germany), the director orientation was perfectly homeotropic.

The thickness of the filled cells was measured by the crystal rotation method [23] with an accuracy of 0.2μm. Optical refractive indices of 5CB were obtained by means of a higher accuracy modification of the prism method using an orienting magnetic field [24].

We then monitored the Fréedericksz transition in our samples. Filled cells were placed in a magnetic field (with LC director perpendicular to the field) between two crossed polars and illuminated with a He-Ne laser (Uniphase, CA). Optical transmission curves were recorded versus magnetic field with an accuracy of 0.5 mT and then converted into optical retardation. Calibration of magnetic field versus current was performed by means of ^{1}H NMR. Sample temperature was maintained to better than 0.1 K.

Finally, we fitted these optical retardation curves, minimizing the difference between experiment and theory [Eq. (11)] of a number of LC cells by variation of K_{33} and K_{11} for all the cells and by separate variation of d (within its error limits, see below) and W_S for every single cell.

RESULTS

Experimental results obtained by the crystal rotation method are illustrated in Fig. 3 by a typical experimental transmission curve together with the theoretical fit. On the assumption that optical refractive indices are known with a high degree of precision and the glass plates of the LC cell are parallel, from the fit in Fig. 3 the thickness of the filled cell can be determined with an accuracy of 0.2 μm.

5CB refractive indices were measured by us at several temperatures and wavelengths. The results are summarized by the following fitted expressions:

$$n_e=\sqrt{1+\frac{a_2}{(1-a_4/\lambda^2)}},\quad n_o=\sqrt{1+\frac{a_1}{(1-a_3/\lambda^2)}},$$

$$\text{with}\quad a_n=D_n\left(1-\frac{T}{T_n}\right)^{e_n},\quad n=1,\ldots,4,$$

where

$$D_1=1.220,\quad T_1=308.32\ \text{K},\quad e_1=-0.010\,38,$$

$$D_2=2.0122,\quad T_2=309.5\ \text{K},\quad e_2=0.045\,57,$$

$$D_3=19\,238.7\ \text{nm}^2,\quad T_3=309.32\ \text{K},\quad e_3=-0.0535,$$

$$D_4=43\,612.1\ \text{nm}^2,\quad T_4=309.0\ \text{K},\quad e_4=0.038\,58.$$

For determination of the value of surface energy W_S, we used 15 LC cells with cell thicknesses between 16 μm and 23 μm. The surfaces of the cells were covered by DPPC monolayer LB films deposited at various surface pressures π, i.e., with varying area A per molecule (see the π-A isotherm on Fig. 5). In Fig. 4, the experimental transmission curve and the calculated optical retardation curve are plotted

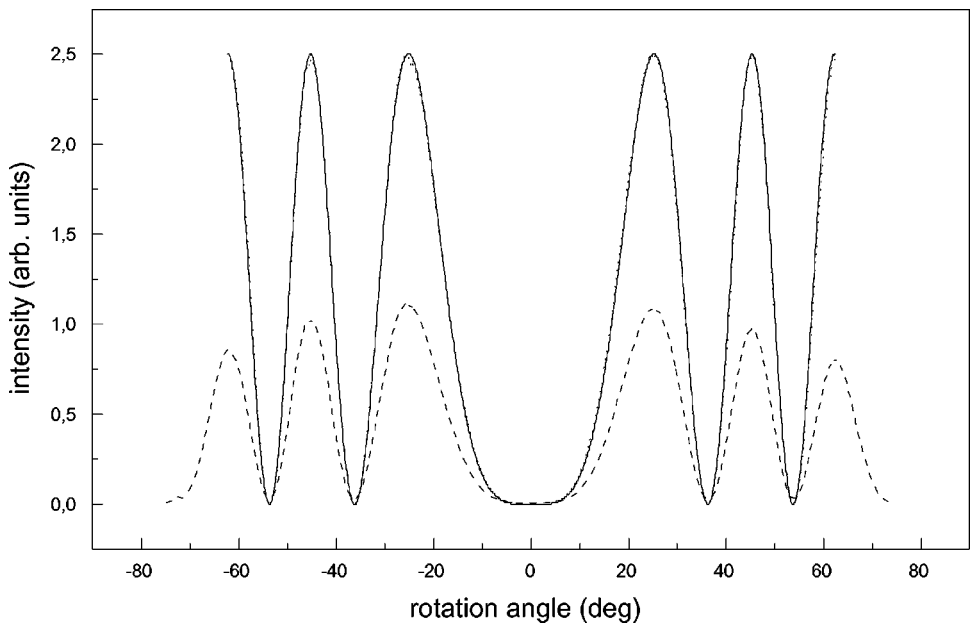

FIG. 3. Determination of the thickness of a filled LC cell by the crystal rotation method. The dashed line is the experimental curve taken at 28.2 °C, the dotted line is the normalized curve, and the solid line is the fit [$d=(27.7\pm0.2)$ μm, $\theta_S=0.04°\pm0.10°$, $\lambda=632.8$ nm)].

vs. applied magnetic field for a 18.6 μm 5CB-DPPC ($A=0.94$ nm^2/molecule) cell at 23 °C, together with the theoretical fit according to Eq. (11). The curvature of the optical retardation curve is mainly determined by the K_{33}/K_{11} ratio. The slope and the Fréedericksz threshold field are most sensitive to surface energy W_S. For the whole set of LC cells we obtained from the fit $K_{33}=10.13$ pN and $K_{11}=8.08$ pN at 23 °C. Data for some other temperatures are given in Table I. Values of W_S for every single cell are shown in Fig. 5 as a function of the area per molecule A. They all correspond to a fairly strong anchoring (extrapolation length is roughly $b=K_{33}/W_S=0.1$ μm). Surprisingly, W_S exhibits a minimum at about $A=0.82$ nm^2/molecule, quite independent of temperature. This unexpected result will be discussed in the section below.

DISCUSSION

In order to discuss the area dependence on anchoring in terms of the coupling model of surface polarization to surface electric field, we need to explicitly relate these two surface properties to monolayer lipid density n_{LB}. Most simple is then to assume that each lipid molecule carries a charge βq_e, where $\beta(\ll 1)$ is the partial charge per lipid head. In such a case the surface electric field will be

$$E_0=\frac{\beta q_e}{\epsilon_{||}\epsilon_0}n_{\mathrm{LB}}. \tag{12}$$

We shall model the area dependence on the surface polarization following the ''hole concept'' (Fig. 1) with the following ansatz:

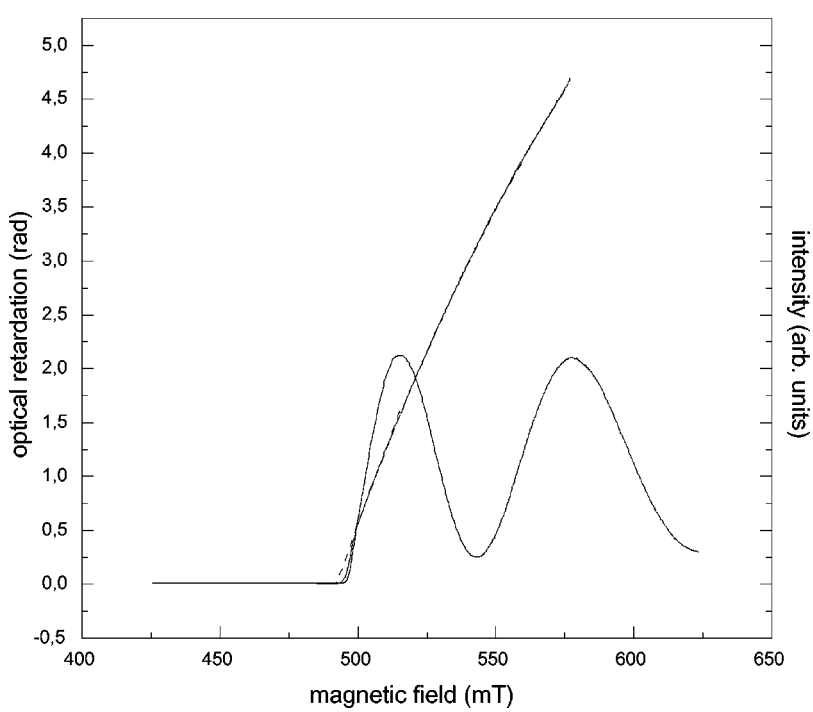

FIG. 4. Optical transmission curve of a 5CB cell between crossed polarizers in dependence of the applied magnetic field, showing maxima and minima; calculated optical retardation curve (solid line) and fitted curve (dashed line) ($\lambda=632.8$ nm, $d=18.6$ μm, $T=23.0$ °C, $A=0.94$ nm^2).

TABLE I. Surface anchoring parameters of 5CB oriented by a DPPC monolayer and bulk elastic constants of 5CB. $W_S^{\min}$ is the minimum value of the surface energy anchoring coefficient occurring at a packing density $n_{\mathrm{LB}}^{\min}$ of the DPPC monolayer. P_{S0} is the surface polarization of 5CB and β is the partial electric charge per lipid molecule in units of proton charge. The standard deviation of $P_{S0}\beta$ ranges from 13% at 23°C to 18% at 33 °C. $W_S^{\min}$, $n_{\mathrm{LB}}^{\min}$, and $P_{S0}\beta$ were obtained from the fit according to Eq. (14). The bend elastic constant, K_{33}, and the splay elastic constant, K_{11}, were extracted from the fit of the optical retardation curves Eq. (11) of all cells of the set.

T (°C)	$W_S^{\min}$ (μJ/m^2)	$n_{\mathrm{LB}}^{\min}$ (nm^{-2})	$P_{S0}\beta$ (pC/m)	K_{33} (pN)	K_{11} (pN)
23	44	1.18	−7.7	10.1	8.1
25	37	1.17	−5.5	9.3	7.8
27	32	1.17	−7.4	8.3	7.2
29	26	1.17	−3.0	7.4	6.6
31	22	1.16	−3.5	5.8	6.2
33	20	1.17	−3.0	4.8	4.6

$$P_S = P_{S0}\left[1 - \frac{n_{\mathrm{LB}}}{n_{\mathrm{LB}}^{\max}}\right], \tag{13}$$

where $n_{\mathrm{LB}}^{\max}$ is the maximum lipid density at close packing (in our case $n_{\mathrm{LB}}^{\max} = 2.22\times 10^{18}$ m^{-2}, corresponding to a minimum area of 0.45 nm^2 from the DPPC isotherm, Fig. 5). In this way surface polarization is linearly related to the total hole area, available for 5CB molecules to penetrate. With Eqs. (12) and (13) in mind, Eq. (7) then takes the form

$$W_S = W_0 + \left(\frac{\Delta\epsilon\epsilon_0 k_B T}{q_e} + e + P_{S0}\right) A n_{\mathrm{LB}} - P_{S0} A \frac{n_{\mathrm{LB}}^2}{n_{\mathrm{LB}}^{\max}}, \tag{14}$$

where $A = \beta q_e/(\epsilon_{||}\epsilon_0)$ and $\epsilon_{||} = 18$ [19]. Equation (14) represents a parabola with a minimum at

$$n_{\mathrm{LB}}^{\min} = \frac{n_{\mathrm{LB}}^{\max}}{2}\left(1 + \frac{e + (k_B T/q_e)\Delta\epsilon\epsilon_0}{P_{S0}}\right), \tag{15}$$

provided $\mathrm{sgn}(P_{S0}\beta) = -1$, i.e., that surface field and polarization are oppositely directed with respect to one another. With a cyanogroup of 5CB molecule facing the surface, polarization will be oriented like the surface normal, i.e., in a positive direction; this means that $\beta < 0$, i.e., surface charge must bear a negative sign.

P_{S0} could be estimated from the longitudinal dipolar moment of 5CB, 16.3×10^{-30} C m [25], or 21.6×10^{-30} C m [26] and the cross section area of a 5CB molecule, 0.4 nm^2

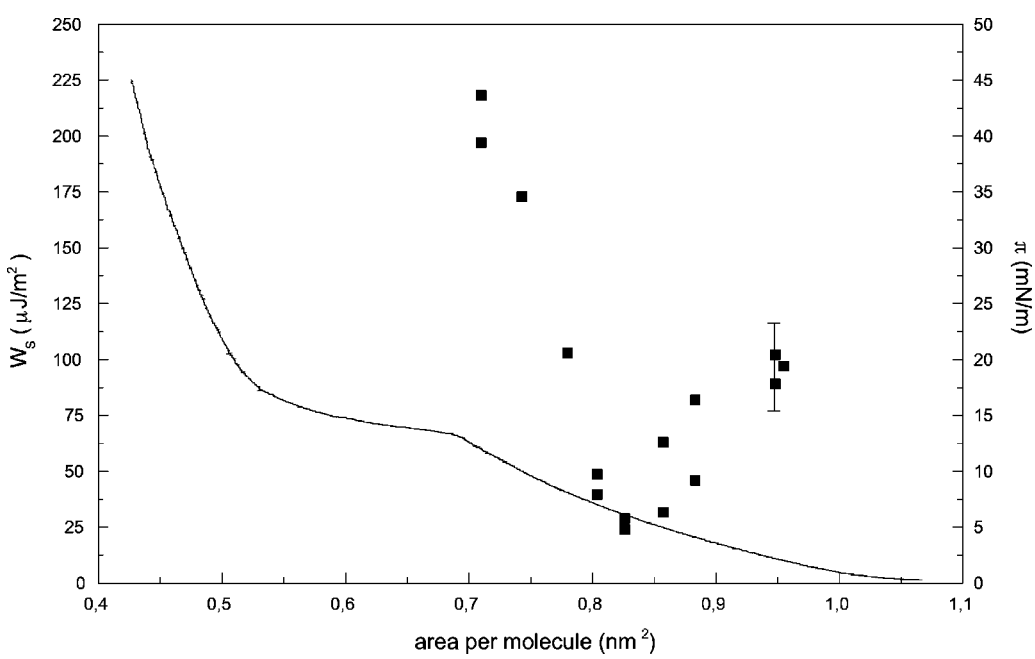

FIG. 5. Surface elastic energy W_S (left-hand side ordinate, standard deviation of the fit indicated by the bar) versus the molecular area A of 15 DPPC-covered LC cells at 23.0 °C. On the same plot a π-A isotherm of the DPPC monolayer at air/water interface for 26 °C (the temperature at which LB film deposition was always affected) is presented (surface pressure π on the right-hand side ordinate).

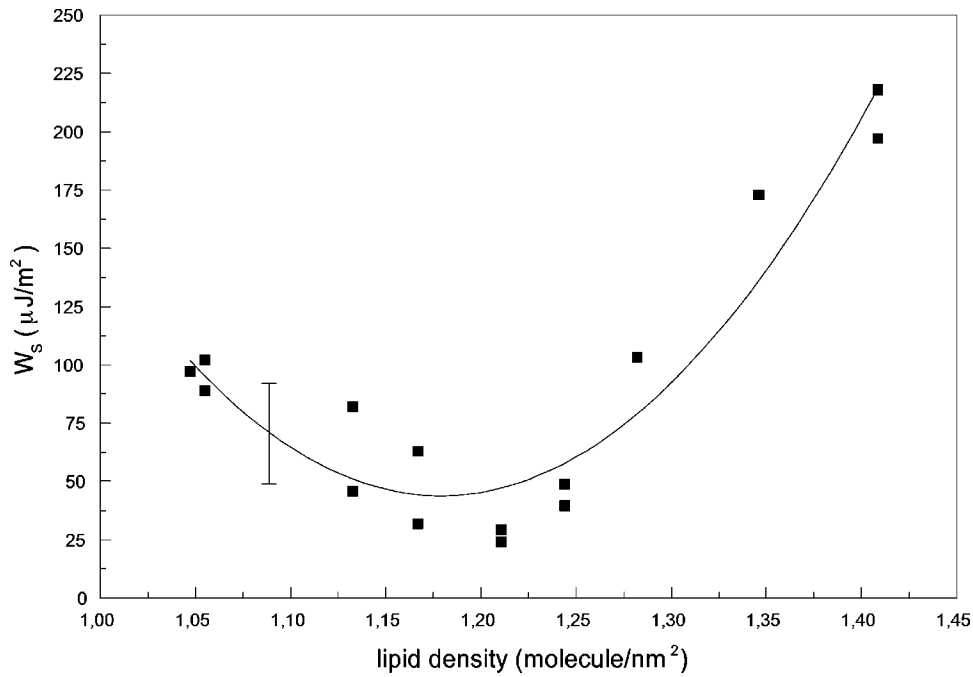

FIG. 6. Second-order polynomial regression of W_S data vs area density n_{LB} for 23.0 °C. The scatter in the measured data (characterized by the standard deviation and indicated by the bar) is mainly caused by the deviation of a fitted curve from the experimental optical retardation curve in the near Fréedericksz threshold (Fig. 4). This deviation depends on the exact adjustment of cells in the magnetic field in connection with the gradual increasing of the external field (in steps of 2.5 mT) in finite time. (A larger experimental Fréedericksz threshold stands for a very good adjustment of cells in the magnetic field, because the relaxation time at the threshold is infinite.) When this part of the experimental curves is neglected in the fitting process, the standard deviation of second-order polynomial regression is decreased (but not done in the presented data).

(the collapse area of a pure 5CB monolayer on water/air interface [6]) as $(4.1–5.4)\times 10^{-11}$ C/m. To account for the larger than a monolayer thickness of the surface polarized layer due to a diffusion of the oriented molecules inside the bulk within about three molecular lengths [14,15], we can triple this value and arrive at $P_{S0}\approx 1\times 10^{-10}$ C/m. If we then neglect the first and the second term in the parentheses of Eq. (14) by reasons explained after Eq. (7) above, we can calculate the partial charge per head β from the parabola's curvature.

The result from a second-order polynomial regression of W_S data at 23 °C is shown in Fig. 6. Data from this and other fits at higher temperatures are given in Table I. Bulk elastic constants, common parameters of all cells obtained by determination of surface energy values, show a decrease with temperature that is familiar for a NLC (let us note that our K_{ii} values are slightly higher than the literature ones, but in general higher values are more reliable than lower ones, since all sample imperfections contribute to a decrease of elastic constants). The temperature-independent position $n_{\mathrm{LB}}^{\min}$ of the W_S minimum justifies the estimation $P_{S0}\approx 1\times 10^{-10}$ C/m permitting to neglect the second term in the large parentheses of Eq. (15); with a lower value of P_{S0} the temperature dependencies of e and $\Delta\epsilon$ would have shown up. This reinforces the dominance of surface interactions over bulk interactions. Indeed, from β at 23° we obtain a value $\lambda_S = 0.6$ nm [Eq. (2)].

Assuming the surface polarization P_{S0} to be independent of temperature and having the value given above, we obtain from column 4 in the table the value β of relative partial charge. These values for the partial charge of DPPC could be favorably compared to some recent findings [27,28], indicating that the PC head group, although zwitterionic (see Ref. [16], p. 356) is weakly negatively charged.

Another possible mechanism of the origin of charge is a lipid-assisted dissociation of some groups on the glass surface and diffusion of the protons to the bulk, leaving the surface negatively charged. In such a case, according to the mass action law, the amount of surface charge is proportional to $\sqrt{n_{\mathrm{LB}}}$, and so is the surface field [cf. Eq. (12)]. In such a case the equivalent of Eq. (15) also corresponds to a curve with a minimum which is, however, shifted to lower film densities. Note, the observed temperature dependence of the product $P_{S0}\beta$ could likely be caused at constant β by a decrease of P_{S0} with temperature.

CONCLUSION

We presented here quantitative measurements of anchoring energy of a nematic liquid crystal on LB film in dependence on film packing density, demonstrating a nonmonotonic behavior of anchoring and a minimum of anchoring energy. The appearance of such a minimum was rationalized within a general theoretical framework of nematic anchoring as mainly due to an electric coupling between surface field and surface polarization of the nematic, both being dependent on LB film surface density.

ACKNOWLEDGMENTS

This work was partially supported by Grant No. SFB 294 of the DFG. One of the authors (A.G.P.) thanks Sächsische Staatsministerium für Wissenschaft und Kunst for support, and the Institut für Experimentelle Physik I, Universität Leipzig, for hospitality. Partial support from the Bulgarian National Fund ''Scientific Studies'' (Project No. F519) was also provided.

[1] J. Cognard, Mol. Cryst. Liq. Cryst. Suppl. Ser. **1**, 1 (1982).
[2] B. Jérôme, Rep. Prog. Phys. **54**, 391 (1991).
[3] K. Hiltrop and H. Stegemeyer, Mol. Cryst. Liq. Cryst. Lett. **49**, 61 (1978).
[4] K. Hiltrop and H. Stegemeyer, Ber. Bunsenges. Phys. Chem. **85**, 582 (1981).
[5] K. Hiltrop, J. Haase, and H. Stegemeyer, Ber. Bunsenges. Phys. Chem. **98**, 209 (1994).
[6] U. Kühnau, B. Mädler, P. Krüger, C. Lautz, G. Rapp, and H. Schmiedel, in *Proceedings of the 26 Freiburger Arbeitstagung, Freiberg, Germany*, edited by G. Strobl (Universitaet Freiburg, Freiburg, 1997), p. 28.
[7] U. Kühnau, B. Mädler, S. Wurlitzer, G. Rapp, and H. Schmiedel, Mol. Cryst. Liq. Cryst. Sci. Technol., Sect. A **304**, 171 (1997).
[8] L. M. Blinov, A. Yu. Kabaenkov, and A. A. Sonin, Liq. Cryst. **5**, 645 (1989).
[9] P. G. de Gennes, *The Physics of Liquid Crystals* (Clarendon, Oxford, 1974).
[10] R. Hirning, W. Funk, H.-R. Trebin, M. Schmidt and H. Schmiedel, J. Appl. Phys. **70**, 4211 (1991).
[11] G. Barbero and G. Durand, J. Appl. Phys. **67**, 2678 (1990).
[12] A. L. Alexe-Ionescu, G. Barbero, and A. G. Petrov, Phys. Rev. E **48**, R1631 (1993).
[13] G. Barbero and A. G. Petrov, J. Phys.: Condens. Matter **6**, 2291 (1994).
[14] A. G. Petrov and A. Derzhanski, Mol. Cryst. Liq. Cryst. Lett. **41**, 41 (1977).
[15] A. Derzhanski and A. G. Petrov, Acta Phys. Pol. A **55**, 747 (1979).
[16] J. N. Israelachvili, *Intermolecular and Surface Forces* 2nd ed. (Academic Press, London, 1992), Chap. 12.
[17] R. N. Thurston, J. Cheng, R. B. Meyer, and G. D. Boyd, J. Appl. Phys. **56**, 263 (1984).
[18] B. Tenchov and J. Brankov, J. Colloid Interface Sci. **109**, 172 (1986).
[19] B. R. Ratna and R. Shashidar, Mol. Cryst. Liq. Cryst. **42**, 113 (1977).
[20] P. R. Maheswara Murthy, V. A. Raghunatan, and N. V. Madhusudana, Liq. Cryst. **14**, 483 (1893).
[21] A. Rapini and M. Papoular, J. Phys. (Paris), Colloq. (Paris) **30**, C4-54 (1969).
[22] B. J. Frisken, J. F. Carolan, and P. Palffi-Muhoray, Mol. Cryst. Liq. Cryst., Lett. Sect. **3**, 57 (1986).
[23] K. Y. Han, T. Miyashita, and T. Ushida, Mol. Cryst. Liq. Cryst. Sci. Technol., Sect. A **241**, 147 (1994).
[24] W. Burkersrode, H. Schmiedel, and H. Schulze, GDR Patent No. 254 069 (1988).
[25] E. Megnassan and A. Proutierre, Mol. Cryst. Liq. Cryst. **108**, 245 (1984).
[26] C. I. Adam, S. I. Clark, G. J. Ackland, and J. Crain, Phys. Rev. E **55**, 5641 (1997).
[27] J. Rädler and E. Sackmann, Langmuir **8**, 848 (1992).
[28] W. Xu, B. L. Blackford, J. G. Cordes, M. H. Jericho, D. A. Pink, V. G. Levadny, and T. Beveridge, Biophys. J. **72**, 1404 (1997).